Science and Technology Indonesia
e-ISSN:2580-4391 *p*-ISSN:2580-4405
Vol. 9, No. 4, October 2024

Research Paper

Isolation and Characterization of Cellulose Nanofibrils (CNF) from Dates by-Product via Citric Acid Hydrolysis

Laaili Azti Rohaadatul Aisy[1], Tetty Kemala[1]*, Lisman Suryanegara[2], Henny Purwaningsih[1]

[1]*Department of Chemistry, Faculty of Mathematics and Natural Science, IPB University, Dramaga, Bogor, 16680, Indonesia*
[2]*Research Center for Biomass and Bioproducts, National Research and Innovation Agency (BRIN), Cibinong, 16911, Indonesia*
***Corresponding author**: tettykemala@apps.ipb.ac.id

Abstract

Industrial residues that are not optimally utilized are removed by burning, landfilling, or dumping, which can threaten the environment and health. In fact, part of this agro-industrial waste still has content that has the potential to become raw material for value-added other industries. Dates by-product as residue of the fiber-rich fruit industry have the potential to be a source of nanocellulose. This study aims to obtain nanofibril cellulose (CNF) isolates from dates by-product via citric acid hydrolysis, and investigate the effect of acid concentration on the unknown dates by-product CNF isolate characteristics. Pretreatment such as delignification and bleaching is needed to obtain cellulose isolate with high purity. Furthermore, acid hydrolysis, centrifugation, and sonication are performed to obtain CNF. CNF isolates are characterized by the analysis of particle size distribution, morphology, and crystallinity. Analysis of functional groups and lignocellulose content test confirm that lignin and hemicellulose are degraded during isolation. The particle size distribution measurement shows that the greater the acid concentration, the smaller the CNF size and the better the size uniformity. The morphology of the CNF obtained is net-like fibers. The degree of crystallinity shown decreases with increasing acid concentration. This study revealed that different citric acid concentrations can result in different characteristics of CNF isolates.

Keywords

Cellulose Nanofibrils, Citric Acid, Concentration, Dates by-Product, Hydrolysis

Received: 4 April 2024, Accepted: 18 June 2024
https://doi.org/10.26554/sti.2024.9.4.818-827

1. INTRODUCTION

Industrial residues as part of agro-industrial waste are defined as residues produced by the food processing industry. The amount of world food crop production reached 9.3 billion tons in 2020, an increase of 52% from 2000 (Food and Agriculture Organization of the United Nations, 2022). Capanoglu et al. (2022) mentioned that almost one-third of food produced becomes waste before and after reaching the consumers. This fantastic value can be a threat to the environment, to human and animal health. Generally, industrial residues are eliminated through burning, landfilling, or dumping, which contributes to several greenhouse gas emissions and potentially exacerbates climate change. About 21-37% of greenhouse gases are produced from the agricultural sector (Lynch et al., 2021). In addition, industrial residues can also be economically detrimental due to the loss of bioactive components and fibers that are beneficial for various industrial sectors. The conversion of industrial residues into value-added materials has been investigated as a means of sustainable resource management, highlighting the new idea of 'bioeconomy' and 'biorefinery', which residue materials from certain industries could be considered as raw materials for other industrial processes.

Based on their content, industrial residues include lignocellulose tertiary sources. Pomace and peels as industrial residues contain 9–18% cellulose, 4–6% hemicellulose, and 3–6% lignin (Khorairi et al., 2021). Dates by-product is a residue in the form of pomace produced from the date palm juice processing industry. Dates as a fiber-rich fruit have a cellulose fraction of 42.5%, hemicellulose 17.5%, and lignin 11.0% (Mrabet et al., 2019; Attia et al., 2021). One of the date palm juice industries in Bogor produces dates by-products of 200 kg/day or 73 tons/year. Based on Attia et al. (2021), dates by-products have been used as poultry feed, but its use is still limited. Cellulose as the main component of lignocellulose has been widely used in various fields, such as the paper industry (Malachowska et al., 2020), packaging (Rahmatullah et al., 2022), adsorbents (Ginting and Mohadi, 2017), biomedicine (Yuwono et al., 2022), sensors (Fan et al., 2020), and cosmetics (Amorim et al., 2021). The potential applications of cellulose are wide because cellulose includes renewable, biodegradable, inexpensive, non-toxic, and biocompatible materials.

Cellulose that has a size of <100 nm at least in one of its dimensions is known as nanocellulose (NC) (Yurdacan and Sari, 2021). Industrial residues that have been used as NC raw materials include grape pomace (Coelho et al., 2018), apple pomace (Wang et al., 2022), rhubarb pomace (Wang et al., 2022), cassava peel (Widiarto et al., 2019), and orange peel (Chen et al., 2024). Generally, NC is used as a reinforcing material in bionanomaterials. This is related to the advantages of its mechanical properties, biocompatibility, surface chemistry, and beneficial optical properties. NC preparations are differentiated into nanocrystalline cellulose (CNC) and nanofibrils (CNF) based on their structural components and dimensions. CNC lengths range from 100–250 nm, while CNF lengths are several micrometers (Blanco et al., 2018). This difference in size can affect the characteristics of nanomaterials and their potential applications. Jadaun et al. (2023) revealed that CNF can form denser networks with polymers than CNC in the application of bio-nanocomposite reinforcing materials.

Cellulose nanofibrils can be isolated through chemical, mechanical, enzymatic, and physicochemical approaches. The physicochemical approach which is a combination of chemical approach (acid hydrolysis) and mechanical approach (sonication) is commonly used because it can minimize dilute acid waste from pure chemical approach and does not require excess energy, which is a drawback of the rigorous mechanical approach. The acid hydrolysis method is influenced by the concentration, temperature, degradation time, and ratio between acid solvent and cellulose. Hydrolysis usually uses inorganic acids such as HCl, H_2SO_4, and H_3PO_4. These acids, especially H_2SO_4, are highly corrosive, environmentally unfriendly, and have the potential to damage nanocellulose isolates due to excessive hydrolysis (Arnata et al., 2020). In addition, the presence of sulfate groups can also decrease the thermal stability of CNF isolates. Liu et al. (2017) isolated NC through citric acid hydrolysis. Citric acid as an organic acid is environmentally friendly, can be recycled through crystallization, and has a low risk of isolate damage. The concentration of citric acid was varied to investigate its effect on the unknown characteristics of CNF isolates from dates by-product.

2. EXPERIMENTAL SECTION

2.1 Materials

Dates by-product was obtained from CV. Sehat Prima Lestari (Bogor-Central Java). All the chemicals used in this study, hydrogen peroxide 30% (H_2O_2) (by Sigma Aldrich), citric acid monohydrate ($C_6H_8O_7{\cdot}H_2O$) (by Supelco Merck), neutral detergent solution (NDS) (by Supelco Merck), acid detergent solution (ADS) (by Supelco Merck), sodium hydroxide (NaOH) (by Supelco Merck), sulphuric acid 96% (H_2SO_4) (by Supelco Merck), acetone ($(CH_3)_2CO$) (by Supelco Merck), and aquadest. The instruments used in this study include Fourier transform infra-Red (FTIR) Perkin Elmer Spectrum One, X-ray diffractometer (XRD) Shimadzu MAXima 7000, particle size analyzer (PSA) Microtrac Nanotrac Wave II, Field Emission Scanning Electron Microscope (FE-SEM) Thermo Scientific Quattro S, High-Resolution Transmissions Electron Microscopy (HR-TEM) Talos F200C, freeze dry Buchi Lyovapor L200, centrifuge Suprema21, and sonicator Qsonica Q2000.

2.2 Isolation of Dates by-Product Cellulose

Dates by-product fiber (DF) cellulose was isolated using the method of Arnata et al. (2020) by modifying the reaction temperature. First, the DF is dried in an oven at 100°C for 24 hours, then mashed using a blender and sifted using a 40 and 100 mesh sieve. DF dry powder was pretreated with a base using 10% NaOH (w/v) 1:10 for 2 hours at 100°C until a solid black mixture was obtained, then filtered using a filter cloth and neutralized with aquadest. The residue of this stage is called dates fiber-delignified (DFD). After that, DFD is bleached using H_2O_2 30% (v/v) 1:20 for 2 hours at 90°C until the mixture is yellowish white, which is called dates fiber-1st bleached (DFB1), then filtered and rinsed again with aquadest until neutral pH. Furthermore, the date pulp was bleached again using a mixture of 30% H_2O_2 (v/v) and 10% NaOH (w/v) 1:2 with a sample ratio and solvent 1:5 for 1 hour at a temperature of 80°C until white. This residue is called dates fiber-2nd bleached (DFB2). The cellulose obtained is dried at 60°C for 3 hours, then weighed, and the yield is calculated. Changes in functional groups of raw materials into cellulose isolates were investigated using FTIR.

2.3 Lignocellulosic Content Test

This method refers to Van Soest et al. (1991). Lignocellulose is a complex biopolymer consisting of cellulose, hemicellulose, and lignin. Lignocellulose levels are tested on the results of each step of the cellulose isolation process. Analysis of hemicellulose levels begins by determining the levels of neutral detergent fiber (NDF) and acid detergent fiber (ADF). NDF analysis starts by inserting a sample of 1 g (M_N) into a 600 mL cup glass, adding 100 mL of neutral detergent solution, and then bringing it to a boil. The sample is extracted for 60 minutes from the start of boiling. The extracted sample is filtered using a pre-weighed filter funnel crucible (M_0). The residue is rinsed with hot reverse osmosis (RO) water and acetone. The filter funnel crucible and residue are dried in a 105°C oven for approximately 4 hours until the weight is constant. After cooling in a desiccator, the cup is weighed (M_1). NDF levels are calculated using Equation 1.

$$\mathrm{NDF}(\%) = \frac{M_1 - M_0}{M_N} \times 100\% \tag{1}$$

ADF analysis begins by inserting 1 g (M_A) sample into a 600 mL cup glass, adding 100 mL of acid detergent solution (ADS), and then bringing it to a boil. The sample is extracted for 60 minutes from the start of boiling. The sample is filtered using a pre-weighed filter funnel crucible (M_0). The residue is rinsed using RO water and acetone. The filter funnel crucible and residue are dried in a 105°C oven for approximately 4 hours until the weight is constant. After cooling in a desiccator, the cup is weighed (M_1). ADF levels are calculated using Equation 2. Hemicellulose levels are calculated by subtracting NDF levels from ADF levels (Equation 3).

$$\mathrm{ADF}(\%) = \frac{M_1 - M_0}{M_N} \times 100\% \tag{2}$$

$$\mathrm{Hemicellulose}(\%) = \mathrm{NDF} - \mathrm{ADF} \tag{3}$$

Cellulose analysis is a continuation of ADF analysis. The sample from ADF analysis that has been weighed (M_1) plus 72% sulfuric acid solution until submerged for 3 hours, then the residue is rinsed with hot RO water and acetone. The residue is dried in a 105°C oven for approximately 4 hours until the weight stabilizes, cooled in a desiccator, and weighed (M_2). The cellulose content is calculated using Equation 4.

$$\mathrm{Cellulose}(\%) = \frac{M_1 - M_2}{M_A} \times 100\% \tag{4}$$

Analysis of lignin levels is a continuation of cellulose analysis. Samples from the analysis of dried cellulose are heated in a furnace with a temperature of about 600°C. The cup is then cooled in a desiccator and weighed (M_3). Lignin levels are calculated using Equation 5.

$$\mathrm{Lignin}(\%) = \frac{M_2 - M_3}{M_A} \times 100\% \tag{5}$$

2.4 Fabrication of Dates by-Product Cellulose Nanofibrils

Nanofibrils cellulose can be further isolated from pre-purified cellulose pulp. The following method refers to Bondancia et al. (2020) without dialysis. First, 4 g of DFB2 was hydrolyzed in 100 mL of citric acid with a concentration variation of 5.5, 6.5, and 7.5 M at 100°C for 6 hours with stirring. The suspension is then centrifuged at a rate of 7500 rpm for 20 minutes and washed repeatedly with demineralized water to neutral pH. The suspension was then sonicated at 50% power in an ice bath for 30 minutes until colloidal. The physical characteristics of CNF isolates from three concentration variations were examined using PSA, FE-SEM, HR-TEM, and XRD.

2.5 Degrees of Crystallinity Analysis

The X-ray diffraction (XRD) profiles of nanofibrils cellulose from various hydrolysis concentrations were analyzed using an OriginPro 8.5. The sample was irradiated with Cu Ka at 40 kV and 30 mA, with the symmetry reflection geometry of the "2θ" range between 10 and 40. The crystallinity index (CrI) was evaluated by Segal method (Segal et al., 1959) as in Equation 6:

$$\mathrm{CrI}\ (\%) = 100 \times \frac{I_{200} - I_{am}}{I_{200}} \tag{6}$$

Description:
I_{200} = intensity of the reflection (200) (2θ = 21–23)
I_{am} = intensity of the amorphous portion of cellulose (2θ = 18)

3. RESULTS AND DISCUSSIONS

3.1 Cellulose Isolate and the Yield

Lignocellulose biomass is arranged as microfibrils containing long-chain cellulose bound to hemicellulose and lignin. Pretreatment is necessary to obtain high-purity cellulose isolates. Based on Figure 1, dates by-product reacted with a base produces a blackish-brown residue as part of the soluble lignin. The bond with the lignin compound is broken by adding a base. In addition to lignin, Prasetia et al. (2018) said NaOH can also dissolve hemicellulose, organic acids, and other ingredients to increase the desired cellulose component. The base pretreatment stage uses 10% NaOH to disrupt the lignocellulose matrix and make the cellulose structure easily accessible. Klemm et al. (1998) mentioned that aqueous alkaline solutions can cause dissolution or at least swelling in lignocellulose structures. Without swelling, further reactions are only possible in the surface layer of cellulose because there is a strong hydrogen interaction between cellulose chains. Swelling and dissolution can occur simultaneously in the reaction medium to increase the accessibility of the hydroxy cellulose group. The molecular level explains that there has been a strong chemical interaction between the hydroxy group of cellulose and the NaOH ion that can break inter- and intramolecular hydrogen bonds. Meanwhile, at the supramolecular level, there is a change in lattice dimensions and chain conformation at the maximum swelling alkaline concentration. The maximum solubility generally coincides with limited swelling at an alkaline concentration of about 10%.

The next stage is bleaching, which can perfect the removal of lignin and hemicellulose until bright white cellulose is obtained (Figure 1). This study went through two bleachings using 30% H_2O_2 and a mixture of 30% H_2O_2 and 10% NaOH. Delignifying agents such as H_2O_2 can remove lignin and hemicellulose without significantly reducing cellulose fibers (Wu et al., 2019) and produce an environmentally friendly and highly efficient bleaching process (Tang and Sun, 2017). In addition, hydrogen peroxide can work optimally in alkaline conditions, or called alkaline hydrogen peroxide (AHP), which has been introduced since 1984. Dutra et al. (2017) said AHP improved the delignification process of lignocellulose biomass.

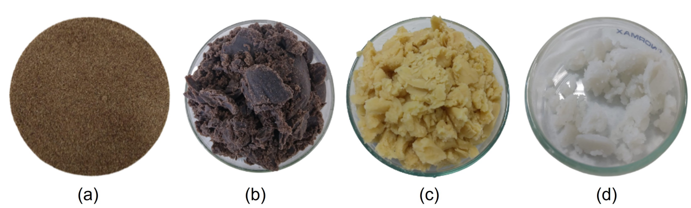

Figure 1. The Physical Appearance of DF (a), DFD (b), DFB1 (c), and DFB2 (d)

The average yield of cellulose isolation from dates by-product with three repetitions reached 8.88 ± 1.42%. This value is relatively low compared to other sources of lignocellulose biomass. The average yield of cellulose isolate of agricultural waste made from cocoa fruit peels, rice straw, coconut husk fiber, and orange peels sequentially was 33.54%, 16.88%, 35.38%, and 66.75% (Lestari et al., 2022; Santhi et al., 2022; Sena et al., 2021; Umaningrum et al., 2018). Arnata et al. (2020) stated that differences in yield values are caused by different types and characteristics of raw materials, type and concentration of solvents, temperature, stirring speed, the ratio between materials and solutions, and reaction time. These parameters are very influential and must be studied for the highest yield and the best characteristics.

3.2 Functional Group Analysis

The success of cellulose isolation from dates by-product was confirmed based on changes in the functional groups of dates by-product fiber as raw material (DF), dates fiber-delignified (DFD), dates fiber-1st bleached (DFB1), and dates fiber-2nd bleached (DFB2) during isolation process. Based on Table 1, date pulp cellulose has an O−H extended vibration in the absorption band ~3333 cm^{-1}. These vibrations occur due to the degradation of hydrogen bonds between cellulose chains during the isolation process. The spectrum shows that there are no lignin and hemicellulose components characterized by absorption bands around 2850, 1733, 1515, and 1235 cm^{-1} as $O-CH_3$, C=O strains, aromatic skeletal C=C vibrations, and aryl−O strains (Figure 2). This is because cellulose isolates have gone through a process of alkaline pretreatment and bleaching. Peaks around 1645–1622 cm^{-1} show deformation of O−H groups due to water absorption by cellulose structures. Arnata et al. (2020) mentioned cellulose is characterized in the absorption band of 1058 cm^{-1} as the C−O−C peak in the cellulose pyranose ring. Meanwhile, absorption bands at around 2918, 1368, and 897 cm^{-1} are C−H extended vibrational peaks, C−H deformations, and glucose ring stretches from cellulose, hemicellulose, and lignin structures.

3.3 Lignocellulosic Content

The method of Van Soest et al. (1991) has been used to determine lignocellulose content. Acid detergent fiber (ADF) mainly consists of cellulose and lignin, while neutral detergent fiber (NDF) has main contents, such as cellulose, hemicellulose, and lignin (Table 2). Cellulose content increases, while lignin and hemicellulose content decrease during the cellulose isolation. The final cellulose isolate of dates by-product reached 90.5% purity. Based on Pinto et al. (2022), cellulose content of >90% indicates high purity of cellulose pulp. This revealed that the isolation stage can increase the purity of cellulose by degrading hemicellulose, lignin, and other ingredients. However, the residual lignin content of DFD is slightly higher than the DF because the method only detects acid-insoluble lignin, so a certain amount of acid-soluble lignin cannot be determined.

Table 2 states that date pulp biomass has a cellulose content

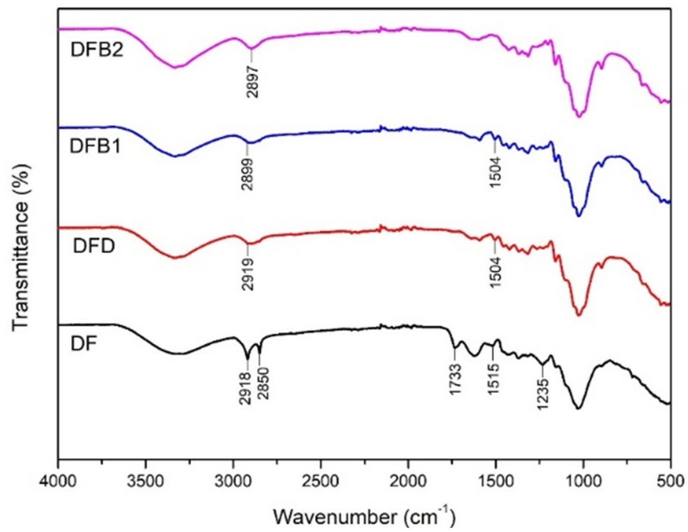

Figure 2. FTIR Spectrum of Cellulose Isolation from Dates by-Product

of 11.0%. This value is lower than the cellulose content of date pulp raw materials reported by Attia et al. (2021), which is 42.5%. The difference can be influenced by where it grows, the type of biomass, the age of plants, plant parts, and environmental factors. Mrabet et al. (2012) also mentioned that different varieties of date palm fruit have different cellulose content, 18.20-24.82%. Furthermore, Table 2 states that the total lignocellulose component is only 54.3%. This is because date dregs, as a by-product of the dates industry, are dominated by sugars, such as glucose, fructose, and sucrose, while fiber only ranges from 2.7-13.8% of the weight of dried dates in various varieties (Ghnimi et al., 2017).

The first and second bleaching in Table 2 showed the same trend, increasing cellulose purity and reducing lignin and hemicellulose levels. However, DFB2 shows a greater value change than DFB1 because alkaline conditions cause hydrogen peroxide to play a more optimal role. Its ability to selectively attack carbonyl and ethylene groups has been shown to improve the delignification process of lignocellulose biomass. According to Dutra et al. (2017), the dissociation of H_2O_2 produces the hydroperoxide anion (HOO^-), which in the alkaline medium HOO^- can react with H_2O_2 again to form superoxide and hydroxyl radicals. The two radicals then carry out chemical attacks on the structure of lignin. Without other reagents, superoxide and hydroxyl radicals can combine and produce oxygen and water.

3.4 Cellulose Nanofibrils Isolate and the Yield

The steps to isolate CNF from dates by-product cellulose pulp include acid hydrolysis, centrifugation, and sonication. Citric acid is used as a hydrolysis agent with the advantages of being environmentally friendly and low risk of damaging CNF isolates (Liu et al., 2017). Citric acid is used with a concentration range of 5.5, 6.5, and 7.5 M and given sample codes CNF-5,

Table 1. FTIR Spectral Vibration from the Cellulose Isolation Processes of Dates by-Product

Possible Peak Assignments	Wavenumber (cm^{-1}) DF	DFD	DFB1	DFB2
O−H stretching of cellulose, hemicellulose, lignin	3333	3335	3336	3335
C−H stretching of cellulose, hemicellulose, lignin	2918	2919	2899	2897
C−H stretching, $O-CH_3$ of lignin	2850	-	-	-
C=O stretching of hemicellulose and lignin	1733	-	-	-
O−H deformation due to absorbed water, oxidation of C–OH groups	1622	1637	1644	1642
C=C aromatic skeletal vibration of lignin	1515	1504	1504	-
C−H deformation of cellulose, hemicellulose, lignin	1368	1368	1368	1368
−OH in-plane bending of cellulose, hemicellulose, lignin	1315	1315	1316	1315
Aromatic ethers, aryl−O stretching of lignin	1235	-	-	-
C−O−C asymmetric stretching of hemicellulose, cellulose, lignin	1155	1158	1156	1157
Alkyl-substituted ether, C−O stretching of cellulose, hemicellulose, lignin	1051	1053	1055	1053
Cyclohexane ring vibrations, skeletal C−C vibrations of cellulose, hemicellulose, lignin	1032	1025	1025	1025
Glucose ring stretching, C_1-H deformation of hemicellulose, cellulose	897	895	895	895
C−OH out-of-plane bending	662	661	660	663

Table 2. Chemical Composition of Each Stage of Cellulose Isolation from Dates by-Product

Material	NDF (%)	ADF (%)	Hemicellulose (%)	Cellulose (%)	Lignin (%)	Total Lignocellulose (%)
DF	60.5	40.8	19.8	11.0	23.6	54.3
DFD	95.5	79.9	15.6	51.0	27.9	94.5
DFB1	98.4	84.3	14.1	60.6	23.2	97.8
DFB2	98.3	93.4	4.8	90.5	2.9	98.2

CNF-6, and CNF-7, respectively. In principle, cellulose acid hydrolysis to obtain CNF involves breaking β-1,4 glycosidic bonds between glucose monomers in cellulose. Meanwhile, centrifugation was carried out repeatedly to neutralize the CNF suspension resulting from acid hydrolysis before sonication. Sonication can produce different cellulose nanofibrils.

CNF colloids were obtained from all three different citric acid concentrations. Such colloids tend to form a gel that does not flow when the vial is turned over. This is thought to be caused by the slight electrostatic repulsion between particles so that it can reduce colloidal stability (France et al., 2017). Bruel et al. (2020) revealed that acid hydrolysis produces charged particles that undergo electrostatic stabilization in highly dielectric solvents like water. In addition, water also has a high chemical affinity for CNF and can be absorbed by its surfaces to form thick layers. The concentration of CNF in the colloid can also affect gel formation. The greater the CNF content in a colloid, the more likely it is to form a gel, and vice versa (Wu et al., 2014).

The highest yield of dates by-product CNF isolation was 60.98% (CNF-7), followed by 51.73% for CNF-5 and 49.15% for CNF-6. This value is relatively high compared to other agricultural waste biomass, such as sago leaves and bagasse, respectively 19% and 35% (Arnata et al., 2020; Pavalaydon et al., 2022). Different types of biomass and isolation conditions can cause a difference in yield. This research shows that the greater the concentration of citric acid used in acid hydrolysis tends to produce an increasing yield. Yu et al. (2012) mentioned that the greater the acid concentration used to hydrolyze cellulose, the higher the CNF yield. However, too high acid concentrations can decrease the yield to extremes because the reaction goes too far and cellulose is completely degraded. This research reveals a smaller CNF-6 yield than CNF-5. It is alleged that there has been a certain amount of CNF loss at the neutralization stage using a centrifuge.

3.5 Size Analysis by PSA

Particle size analyzer (PSA) with dynamic light scattering (DLS) method is used to determine the mean and particle size distribution of cellulose nanofibril isolates. Measuring the size distribution of CNF is challenging because of its irregular net-shaped morphology, wide size distribution, and strong tendency to aggregate or clump. By definition, nanocellulose has a size of <100 nm in at least one of its dimensions. CNF isolated by 7.5 M citric acid hydrolysis had the highest cumulative percent for the presence of a particle size <100 nm. This is due to acid hydrolysis treatment of cellulose, causing some amorphous areas to degrade. Thus, the greater the concentration of acid

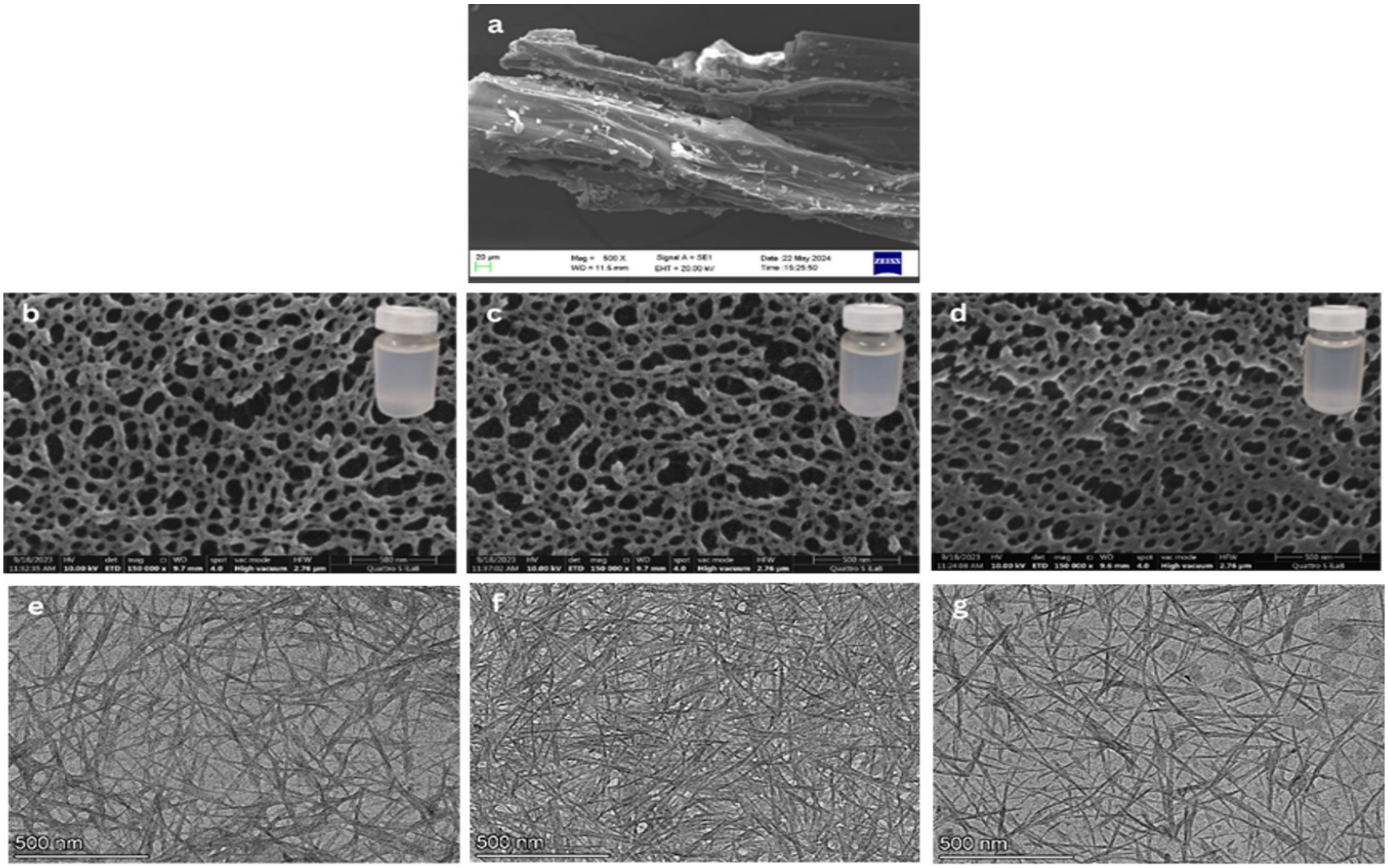

Figure 3. Morphological Characterization: SEM Image of Date Pulp Fiber at 500× Magnification (a), SEM (b-d) and TEM (e-g) Images of CNF at 150,000× and 37,000× Magnification from Three Variations in Acid Concentration 5.5 M, 6.5 M, and 7.5 M

used, the effect on the smaller the size of the CNF (Rana et al., 2023).

Table 3 shows the CNF-7 isolate as the smallest average particle size. The mean size is the value of Mn or mean number diameter, defined as a distribution of numbers calculated using volume distribution data on small particles. In addition, the polydispersity index (PDI) value also shows that CNF-7 has the smallest PDI value. PDI is a representation of the distribution of population size in a given sample. The numerical value of PDI ranges from 0.0 (for perfectly homogeneous samples) to 1.0 (for samples with double particle size populations). Danaei et al. (2018) said PDI ≤0.2 is often considered acceptable for application as polymer-based nanoparticle materials. Based on this statement, CNF-7 has the potential to be applied as a nanocomposite with a PDI value of 0.17. Based on the smallest PDI value, it can also be interpreted that cellulose nanofibrils isolated using 7.5 M citric acid hydrolysis produce the narrowest particle size distribution width. Meanwhile, Jakubek et al. (2018) revealed that determining particle size distribution through the DLS method does not provide particle length or diameter information but measures all types of particles, including individual CNF, aggregates, and agglomerates.

Table 3. Mean Number of Particle Size and Polydispersity Index

Sample Code	Mean Number Diameter (nm)	PDI
CNF-5	63.60	0.42
CNF-6	56.30	0.31
CNF-7	31.80	0.17

3.6 Morphology and Dimensions

The morphology of CNF can be identified using FE-SEM and HR-TEM, and its fiber diameter size distribution is analyzed using ImageJ and OriginPro 8.5 software. This study also observed changes in sample morphology before and after isolation. Date pulp powder shows a large fiber structure with a corrugated surface (Figure 3a). Meanwhile, all CNFs obtained show a smaller fiber and uniformly interconnected net-like fiber structure (Figure 3b-g) with slight differences in diameter size. The morphology is similar to nanocellulose obtained from date palm leaves through 60 wt% sulfuric acid hydrolysis and sonication, with better image resolution (Alhamzani and

Habib, 2021). The bundles formed specifically in Figure 3d show the agglomeration of fibrils. Agglomeration of individual nanofibrils leads to the formation of thicker fibrils. Barbash et al. (2016) predicted the formation of agglomerates caused by strong interactions between particles due to chemical modification of cellulose macromolecules during acid hydrolysis at higher acid concentrations and due to Van der Waals attraction forces between nanofibrils.

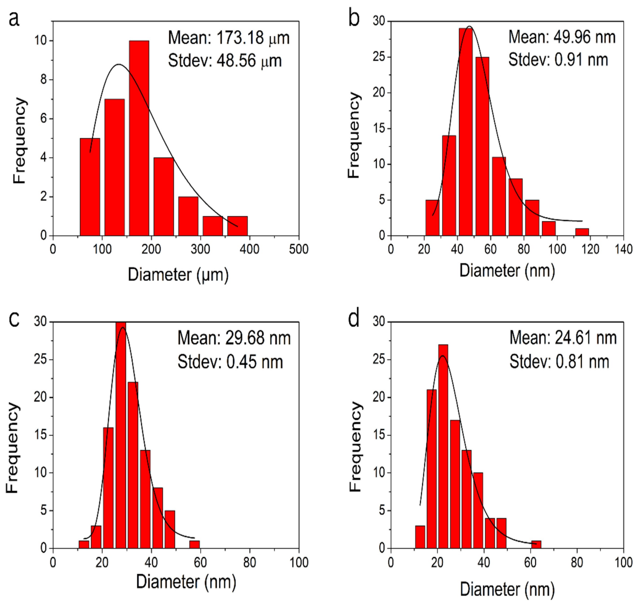

Figure 4. Diameter Distribution of Date Pulp Fiber (a) and CNF from Three Variations in Acid Concentration: 5.5 M (b), 6.5 M (c), and 7.5 M (d)

Based on Figure 4, the isolation process can reduce the fiber size of the raw material, and increasing the acid concentration can reduce the fiber diameter. Higher acid concentrations can produce more active hydronium ions, increasing the degradation of bonds between fibers starting from amorphous structures and producing fibers with shorter diameters. The change in the length of the CNF is also similar to the change in diameter. The length of CNF hydrolyzed with 7.5 M citric acid can be determined as 492.75 ± 238.37 nm. Meanwhile, hydrolysis with smaller concentrations of acids results in lengths that are difficult to determine the endpoint of it due to their relatively long size. The length/diameter ratio of CNF-7 reaches 20.02, or more than 10, so it has the potential to produce a strengthening effect on the composite matrix (Azeredo et al., 2009). This is in line with Mirzaee et al. (2023), who have isolated CNFs with different concentrations of sulfuric acid. In addition to changes in diameter, acid concentration can affect the color of cellulose dispersion in water. Based on Figure 4b-d in the upper right corner, the suspension color appears slightly brown as the concentration of citric acid increases. Arnata et al. (2020) mentioned that at high concentrations, further hydrolysis of cellulose into glucose monomers can occur, which can undergo a browning process. Meanwhile, the study showed that about 8 wt% of water-dispersed CNF had a transparent homogeneous gel form. Due to the ultrasonic disintegration of the cellulose suspension, the stability of the aqueous dispersion increases.

3.7 Degree of Crystallinity

The degree of crystallinity of CNF can be calculated from the XRD diffractogram using the Segal equation. The CI percentage is the ratio of the crystal area to the amorphous. The sample has diffraction peaks at 2θ, 16° and 22°. Segal method uses I_{200} as the main diffraction peak associated with the crystallography field of cellulose I_{200} at 2θ 22.2-22.4° and I_{am} associated with the amorphous phase at 2θ 18.0°. Based on Figure 5, delignification, bleaching, and acid hydrolysis can increase the %CI of cellulose from the raw material, and citric acid hydrolysis with a concentration of 5.5 M has the highest degree of crystallinity at 66.9%. Citric acid concentration of more than 5.5 M can reduce the degree of crystallinity of CNF made from dates by-product. This is because too high acid concentrations can damage the cellulose crystal area. However, the crystallinity of CNF made from dates by-product is still in the crystallinity range of other agro-industrial residue sources, which is 65.0-75.0% (Mariño et al., 2021). Hosseini et al. (2018) obtained CNF from date palm rachis and leaflets through TEMPO treatment and ball mill with crystallinity degree 66.7-68.0%.

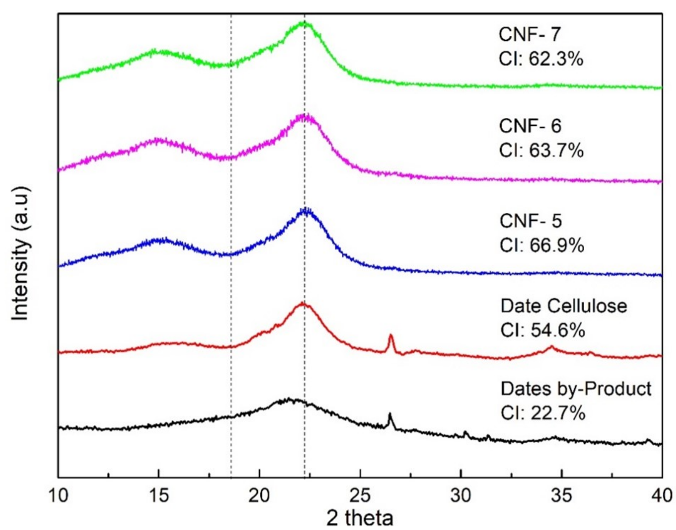

Figure 5. The Diffractogram of Date Pulp Fiber and CNF Based on Variations in Citric Acid Concentration

4. CONCLUSIONS

Cellulose nanofiber (CNF) isolates have been successfully obtained from dates by-product through a physicochemical approach combining citric acid hydrolysis and sonication methods with the highest yield of 60.98%. The cellulose component in date pulp isolate reaches 90.5%. FTIR analysis and lignocellulose content test confirm that lignin and hemicellulose are degraded during isolation. The average fiber diameter obtained was 24.6-50.0 nm based on morphological analysis and 31.8-63.6 nm based on PSA with a polydispersity index below 0.5. The morphology of CNF is interconnected net-like fiber. The degree of crystallinity based on the XRD diffractogram is in the range of 62.3-66.9%. The citric acid concentration of 7.5 M in this study produced the lowest average particle size, the best size uniformity, and the highest yield, so it has the potential for further application as a nanomaterial-based polymer composite.

5. ACKNOWLEDGMENT

The authors acknowledge the facilities, scientific and technical support from Advanced Characterization Laboratories Cibinong–Integrated Laboratory of Bioproduct, National Research and Innovation Agency through E-Layanan Sains, Badan Riset dan Inovasi Nasional.

REFERENCES

Alhamzani, A. G. and M. A. Habib (2021). Preparation of Cellulose Nanocrystals from Date Palm Tree Leaflets (*Phoenix dactylifera* L.) via Repeated Chemical Treatments. *Cellulose Chemistry and Technology*, **55**(1–2); 33–39

Amorim, J. D. P., H. A. Nascimento, C. J. G. S. Junior, A. D. M. Medeiros, I. D. L. Silva, A. F. S. Costa, G. M. Vinhas, and L. A. Sarubbo (2021). Obtainment of Bacterial Cellulose with Added Propolis Extract for Cosmetic Applications. *Polymer Engineering and Science*, **62**(2); 565–575

Arnata, I. W., S. Suprihatin, F. Fahma, N. Richana, and T. C. Sunarti (2020). Cationic Modification of Nanocrystalline Cellulose From Sago Fronds. *Cellulose*, **27**(6); 3121–3141

Attia, A. I., F. M. Reda, A. K. Patra, S. S. Elnesr, Y. A. Attia, and M. Alagawany (2021). Date (*Phoenix dactylifera* L.) By-Products: Chemical Composition, Nutritive Value And Applications In Poultry Nutrition, An Updating Review. *Animals*, **1**(4); 1133

Azeredo, H. M. C., L. H. C. Mattoso, D. Wood, T. G. Williams, R. J. Avena-Bustillos, and T. H. McHugh (2009). Nanocomposite Edible Films from Mango Puree Reinforced with Cellulose Nanofibers. *Journal of Food Science*, **74**(5); 31–35

Barbash, V. A., O. V. Yaschenko, S. V. Alushkin, A. S. Kondratyuk, O. Y. Posudievsky, and V. G. Koshechko (2016). The Effect of Mechanochemical Treatment of the Cellulose on Characteristics of Nanocellulose Films. *Nanoscale Research Letters*, **11**; 410

Blanco, A., M. C. Monte, C. Campano, A. Balea, N. Merayo, and C. Negro (2018). Nanocellulose for Industrial Use: Cellulose Nanofibers (CNF), Cellulose Nanocrystals (CNC), and Bacterial Cellulose (BC). In *Handbook of Nanomaterials for Industrial Applications*. Elsevier

Bondancia, T. J., J. de Aguiar, G. Batista, A. J. G. Cruz, J. M. Marconcini, L. H. C. Mattoso, and C. S. Farinas (2020). Production of Nanocellulose Using Citric Acid in a Biorefinery Concept: Effect of the Hydrolysis Reaction Time and Techno-Economic Analysis. *Industrial & Engineering Chemistry Research*, **59**(25); 11505–11516

Bruel, C., T. S. Davies, P. J. Carreau, J. R. Tavares, and M. C. Heuzey (2020). Self-assembly Behaviors of Colloidal Cellulose Nanocrystals: A Tale of Stabilization Mechanisms. *Journal of Colloid and Interface Science*, **574**; 399–409

Capanoglu, E., E. Nemli, and F. Tomas-Barberan (2022). Novel Approaches in the Valorization of Agricultural Wastes and their Applications. *Journal of Agricultural and Food Chemistry*, **70**(23); 6787–6804

Chen, L., Y. Wu, Y. Guo, X. Yan, W. Liu, and S. Huang (2024). Preparation and Characterization of Soluble Dietary Fiber Edible Packaging Films Reinforced by Nanocellulose from Navel Orange Peel Pomace. *Polymers*, **16**(3); 315

Coelho, C. C. S., M. Michelin, M. A. Cerqueira, C. Goncalves, R. V. Tonon, L. M. Pastrana, O. Freitas-Silva, A. A. Vicente, L. M. C. Cabral, and J. A. Teixeira (2018). Cellulose Nanocrystals from Grape Pomace: Production, Properties and Cytotoxicity Assessment. *Carbohydrate Polymers*, **195**; 327–336

Danaei, M., M. Dehghankhold, S. Ataei, F. H. Davarani, R. Javanmard, A. Dokhani, S. Khorasani, and M. R. Mozafari (2018). Impact of Particle Size and Polydispersity Index on the Clinical Applications of Lipidic Nanocarrier Systems. *Pharmaceutics*, **10**(2); 57

Dutra, E. D., F. A. Santos, B. R. A. Alencar, A. L. S. Reis, R. F. R. de Souza, K. A. S. Aquino, M. A. M. Jr, and R. S. C. Menezes (2017). Alkaline Hydrogen Peroxide Pretreatment of Lignocellulosic Biomass: Status and Perspectives. *Biomass Conversion and Biorefinery*, **8**(1); 1–10

Fan, J., S. Zhang, F. Li, and J. Shi (2020). Cellulose-based Sensors for Metal Ions Detection. *Cellulose*, **27**; 5477–5507

Food and Agriculture Organization of the United Nations (2022). *World Food and Agriculture - Statistical Yearbook 2022*

France, K. J. D., T. Hoare, and E. D. Cranston (2017). Review of Hydrogels and Aerogels Containing Nanocellulose. *Chemistry of Materials*, **29**; 4609–4631

Ghnimi, S., S. Umer, A. Karim, and A. Kamal-Eldin (2017). Date Fruit (*Phoenix dactylifera* L.): An Underutilized Food Seeking Industrial Valorization. *NFS Journal*, **6**; 1–10

Ginting, S. K. and R. Mohadi (2017). Adsorption of Congo Red Using Kaolinite-Cellulose Adsorbent. *Science and Technology Indonesia*, **2**(2); 29–36

Hosseini, M., H. Z. Dizaji, M. Taghavi, and A. A. Babaei (2018). Extraction of Cellulose Nanofibril (CNF) from Agricultural Residues. In *Proceedings of the 7th International Conference on Nanostructures (ICNS7)*

Jadaun, S., U. Sharma, R. Khapudang, and S. Siddiqui (2023). Biodegradable Nanocellulose Reinforced Biocomposites for Food Packaging – A Narrative Review and Future Perspective. *Journal of Water and Environmental Technology*, **8**(3); 293–319

Jakubek, Z. J., M. Chen, M. Couillard, T. Leng, L. Liu, S. Zou, U. Baxa, J. D. Clogston, W. Y. Hamad, and L. J. Johnston (2018). Characterization Challenges for a Cellulose Nanocrystal Reference Material: Dispersion and Particle Size Distributions. *Journal of Nanoparticle Research*, **20**(98); 1–16

Khorairi, A. N. S. A., N. Sofian-Seng, R. Othaman, H. A. Rahman, N. S. M. Razali, S. J. Lim, and W. A. W. Mustapha (2021). A Review on Agro-industrial Waste as Cellulose and Nanocellulose Source and Their Potentials in Food Applications. *Food Reviews International*, **39**(2); 663–688

Klemm, D., B. Phillipp, T. Heinze, and W. Wagenknecht (1998). *Comprehensive Cellulose Chemistry: Fundamentals and Analytical Methods*. Wiley

Lestari, Y. P. I., Y. Falya, U. Chasanah, D. W. Kusumo, and M. Bethasari (2022). Isolation of α-Cellulose, Manufacture & Characterization of Microcrystalline Cellulose (MCC) from Baby Orange Peel Waste (*Citrus sinensis*). *Pharmaceutical and Pharmacology Magazine*, **26**(3); 119–123

Liu, C., H. Du, G. Yu, Y. Zhang, Q. Kong, B. Li, and X. Mu (2017). Simultaneous Extraction of Carboxylated Cellulose Nanocrystals and Nanofibrils via Citric Acid Hydrolysis – A Sustainable Route. *Paper and Biomaterial*, **2**(4); 19–26

Lynch, J., M. Cain, D. Frame, and R. Pierrehumbert (2021). Agriculture's Contribution to Climate Change and Role in Mitigation is Distinct From Predominantly Fossil CO_2-Emitting Sectors. *Frontiers in Sustainable Food Systems*, **4**(518039); 1–9

Malachowska, E., M. Dubowik, A. Lipkiewicz, K. Przybysz, and P. Przybysz (2020). Analysis of Cellulose Pulp Characteristics and Processing Parameters for Efficient Paper Production. *Sustainability*, **12**(17); 7219

Mariño, M. A., D. Cypriano, and L. Tasic (2021). Agroindustry Residues as a Source for Cellulose Nanofibers Production. *Journal of Brazilian Chemical Society*, **32**(4); 878–888

Mirzaee, N., M. Nikzad, R. Battisti, and A. Araghi (2023). Isolation of Cellulose Nanofibers from Rapeseed Straw via Chlorine-Free Purification Method and its Application as Reinforcing Agent in Carboxymethyl Cellulose-Based Films. *International Journal of Biological Macromolecules*, **251**; 126405

Mrabet, A., H. Hammadi, R. Rodríguez-Arcos, A. Jimenez-Araujo, and M. Sindic (2019). Date Palm Fruits as a Potential Source of Functional Dietary Fiber: A Review. *Food Science and Technology Research*, **25**(1); 1–10

Mrabet, A., R. Rodríguez-Arcos, R. Guillen-Bejarano, N. Chaira, A. Frechichi, and A. Jimenez-Araujo (2012). Dietary Fiber from Tunisian Common Date Cultivars (*Phoenix dactylifera* L.): Chemical Composition, Functional Properties, and Antioxidant Capacity. *Journal of Agricultural and Food Chemistry*, **60**; 3658–3664

Pavalaydon, K., H. Ramasawmy, and D. Surroo (2022). Comparative Evaluation of Cellulose Nanocrystals from Bagasse and Coir Agro Wastes for Reinforcing PVA Based Composites. *Environment, Development and Sustainability*, **24**; 9963–9984

Pinto, E., W. N. Aggrey, P. Boakye, G. Amenuvor, Y. Sokama-Neuyam, M. K. Fokuo, H. Karimaie, K. Sarkodie, C. D. Adenutsi, S. Erzuah, and M. A. D. Rockson (2022). Cellulose Processing from Biomass and its Derivatization into Carboxymethylcellulose: A Review. *Scientific African*, **15**; e01078

Prasetia, I. G. N. J. A., S. Deviana, T. Damayanti, A. Cahyadi, and I. M. A. G. Wirasuta (2018). The Effect of NaOH Concentration in Delignification Process on Microcrystalline Cellulose from Green Algae (*Cladophora sp.*) as the Renewable Marine Product. *Journal of Pharmaceutical Science and Society*, **15**(2); 68–71

Rahmatullah, R., K. Putri, M. Rendana, U. Waluyo, and T. Andrianto (2022). Effect of Plasticizer and Concentration on Characteristics of Bioplastic Based on Cellulose Acetate from Kapok (*Ceiba pentandra*) Fiber. *Science and Technology Indonesia*, **7**(1); 73–83

Rana, M. S., M. A. Rahim, M. P. Mosharraf, M. F. K. Tipu, J. A. Chowdhury, M. R. Haque, S. Kabir, M. S. Amran, and A. A. Chowdhury (2023). Morphological, Spectroscopic and Thermal Analysis of Cellulose Nanocrystals Extracted from Waste Jute Fiber by Acid Hydrolysis. *Polymers*, **15**; 1530

Santhi, M., I. W. Arnata, and L. P. Wrasiati (2022). Isolation of Cellulose from Coconut Fiber (*Cocos nucifera* L.) at Variation of Temperature and Time of Bleaching Process with Peracetic Acid. *Journal of Agroindustrial Engineering and Management*, **10**(3); 248–258

Segal, L., J. J. Creely, A. E. J. Martin, and C. M. Conrad (1959). An Empirical Method for Estimating the Degree of Crystallinity of Native Cellulose Using the X-Ray Diffractometer. *Textile Research Journal*, **29**; 786–794

Sena, P. W., G. P. G. Putra, and L. Suhendra (2021). Characterization of Cellulose from the Skin of Cocoa Fruit (*Theobroma Cacao* L.) at Various Concentrations of Hydrogen Peroxide and Bleaching Process Temperatures. *Journal of Agroindustrial Engineering and Management*, **9**(3); 288–299

Tang, P. and G. Sun (2017). Generation of Hydroxyl Radicals and Effective Whitening of Cotton Fabrics by H_2O_2 Under UVB Irradiation. *Carbohydrate Polymers*, **160**; 153–162

Umaningrum, D., R. Nurmasari, M. D. Astuti, M. Mardhatillah, A. Mulyasuryani, and D. Mardiana (2018). Isolation of Cellulose from Rice Straw Using Variations in Base Concentration. *Journal of Science and Applied Chemistry*, **12**(1); 25

Van Soest, P. J., J. B. Robertson, and B. A. Lewis (1991). Methods for Dietary Fiber Neutral Detergent Fiber, and Nonstarch Polysaccharides in Relation to Animal Nutrition. *Journal Dairy Science*, **74**; 3583–3597

Wang, T., J. Jung, and Y. Zhao (2022). Isolation, Characterization, and Applications of Holocellulose Nanofibers From Apple and Rhubarb Pomace Using Eco-Friendly Approach. *Food and Bioproducts Processing*, **136**; 166–175

Widiarto, S., E. Pramono, Suharso, A. Rochliadi, and I. M. Arcana (2019). Cellulose Nanofibers Preparation from Cassava Peels via Mechanical Disruption. *Fibers*, **7**(5); 44

Wu, Q., Y. Meng, S. Wang, Y. Li, S. Fu, L. Ma, and D. Harper

(2014). Rheological Behavior of Cellulose Nanocrystal Suspension: Influence of Concentration and Aspect Ratio. *Journal of Applied Polymer Science*, **131**(15); 40525

Wu, Y., J. Wu, F. Yang, C. Tang, and Q. Huang (2019). Effect of H_2O_2 Bleaching Treatment on the Properties of Finished Transparent Wood. *Polymers*, **11**(5); 776

Yu, M., R. Yang, L. Huang, X. Cao, F. Yang, and D. Liu (2012). Preparation and Characterization of Bamboo Nanocrystalline Cellulose. *BioResources*, **7**(2); 1802–1812

Yurdacan, H. M. and M. M. Sari (2021). *Sustainable Materials for Transitional and Alternative Energy*. Gulf Professional Publishing

Yuwono, S. D., R. Nahrowi, A. Setiawan, N. L. G. R. Juliasih, I. Sukmana, W. Simajuntak, and S. Hadi (2022). Synthesis of Cellulose–Polylactic Acid Microcapsule as a Delivery Agent of Rifampicin. *Science and Technology Indonesia*, **7**(3); 263–268

